Microphase Separation Kinetics in Segmented Polyurethanes: Effects of Soft Segment Length and Structure

**Benjamin Chu,*,†,‡ Tong Gao,† Yingjie Li,† Jian Wang,†
C. Richard Desper,§ and Catherine A. Byrne§**

Department of Chemistry, State University of New York at Stony Brook, Long Island, New York 11794-3400, Department of Materials Science and Engineering, State University of New York at Stony Brook, Long Island, New York 11794, and U.S. Army Materials Technology Laboratory, Watertown, Massachusetts 02172-0001

Received March 9, 1992; Revised Manuscript Received June 9, 1992

ABSTRACT: Synchrotron small-angle X-ray scattering (SAXS) was used to investigate the microphase structure and microphase separation kinetics of two segmented polyurethanes with 4,4′-diphenylmethyl diisocyanate (MDI) and 1,4′-butanediol (BD) as the hard segment and poly(tetramethylene oxide) (PTMO) and poly(propylene oxide) end-capped with poly(ethylene oxide) (PPO–PEO) ($M_n \sim 2000$) as the soft segments. A more complete phase separation was observed in the PTMO based sample although PTMO and PPO–PEO have almost identical solubility parameters. This phase separation behavior could be explained as due partially to a kinetic factor. The microphase separation kinetics from quenching a sample in the melt state to lower annealing temperatures could be described by a relaxation process. A single-relaxation time process was observed for the PTMO based sample. By variation of the soft segment molecular weight from 1000 to 2000, the relaxation time was reduced from $\sim 10^3$ to 64 s. This behavior strongly supports our argument that in a segmented polyurethane, hard segment mobility, system viscosity, and hard segment interactions are the three controlling factors. In the PPO–PEO-based sample a double-relaxation time process was observed. One of the relaxation times was 54 s while the other secondary process was 1.48×10^3 s.

Introduction

Phase separation takes place in segmented polyurethanes due to the thermodynamic incompatibility between the hard and soft segments.[1] However, the presence of chemical linkage between the hard and soft segments restricts the phase structure to the microscale, i.e., on the order of 10 nm. The phase structure is directly responsible for many of the unique mechanical properties in this class of materials.

In early publications,[1] the phase-separated structure was studied mostly from the thermodynamic viewpoint. Recently, we[2-6] have reported on the effects of the kinetic factor on the phase structure. One of the main conclusions is that besides the thermodynamic factor, hard segment mobility, system viscosity, and hard segment interactions are the three controlling factors for the phase structure formation.

Wilkes and co-workers[7-9] were the first to study the time dependence of the structure and properties of segmented polyurethanes by using differential scanning calorimetry (DSC), SAXS, and mechanical testing after the samples were thermally annealed at 170 °C. The results showed a long recovery time. However, their work differs from our present study in two respects. We do not know whether annealing at 170 °C could make the system completely homogeneous. Furthermore, their SAXS data on the time dependence were measured only at a fixed scattering angle. The DSC results by Kwei[10] showed that the phase separation proceeded logarithmically with elapsed time. The separation of soft and hard segments was relatively fast while the ordering of hard segments took a longer time. A similar logarithm relation was found by Camberlin and Pascault.[11] Chee and Farris[12] proposed first-order kinetics for segmented polyurethanes. Application of their theory to earlier experimental results showed two elementary steps which could be described by two relaxation times. Lee et al.[13,14] used Fourier transform infrared spectroscopy (FTIR) and DSC to study the phase separation kinetics of their model segmented polyurethanes. An Avrami equation was used to fit the data. They concluded that phase separation proceeded by a nucleation and growth mechanism with a two-dimensional growth initially followed by a diffusion-dominated mechanism. However, their samples were annealed at 130 °C before being quenched. We do not know whether such a low temperature could create a completely homogeneous state. Galambos et al.[15] were the first to use synchrotron SAXS and wide-angle X-ray diffraction (WAXD) to study the phase separation as well as the crystallization kinetics of their samples. They found that their data could be described by the Avrami equation. However, although they started from a homogeneous melt, they were unable to quench (cool the sample at a fast enough rate so that structural development was negligible during the cooling process) the melt to annealing temperatures due to instrumental limitation; the maximum controlled cooling rate was only 20 °C/min. This cooling rate might not be fast enough to freeze the fast kinetics of their samples. In a previous study,[3] we used synchrotron SAXS to study the phase separation kinetics of a segmented polyurethane with 4,4′-diphenylmethyl diisocyanate (MDI) and 1,4′-butanediol (BD) as the hard segment (MDI/BD) and poly(tetramethylene oxide) (PTMO) end-capped with poly(propylene oxide) (PPO) ($M_n \sim 1000$, PTMO:PPO = 70:30 (wt)) as the soft segments (PPO–PTMO). The kinetics was very slow at most of the temperatures, owing to the high system viscosity and low hard segment mobility, and could be described essentially by an equation of relaxation with a single-relaxation time. According to our mobility–viscosity–interaction argument, if the soft segment length was increased from 1000 to 2000, the reduction in the degree of connectivity between the hard and soft segments (assuming equal molecular weight of the samples) should

* To whom all correspondence should be addressed at the Department of Chemistry, State University of New York.
† Department of Chemistry, State University of New York.
‡ Department of Materials Science and Engineering, State University of New York.
§ U.S. Army Materials Technology Laboratory.

0024-9297/92/2225-5724$03.00/0

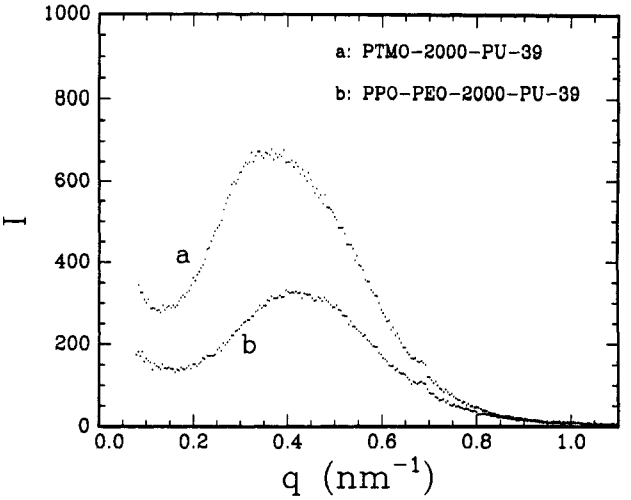

Figure 1. SAXS patterns of as-reacted PTMO-2000-PU-39 and PPO-PEO-2000-PU-39 samples.

make the phase separation process faster. Furthermore it should also be interesting to see which equation is more appropriate to depict the observed phase separation kinetics.

Experimental Section

Materials. Two segmented polyurethanes were used in this study. The hard segment was MDI/BD in both samples. One of the soft segments was PTMO with a number-average molecular weight of about 2000. The other one was PPO end-capped with poly(ethylene oxide) (PPO–PEO) with wt % of PPO:PEO = 55:45 and a number-average molecular weight of about 2000. The molar ratio of PTMO(PPO-PEO):MDI:BD = 1:4:3. The samples, synthesized by a two-step bulk polymerization process, were denoted as PTMO-2000-PU-39 and PPO-PEO-2000-PU-39, respectively, with 39 being the wt % of the hard segment content.

Instrumentation. Synchrotron SAXS measurements were carried out at the SUNY X3A2 beamline, National Synchrotron Light Source (NSLS), Brookhaven National Laboratory (BNL). Details about the instrumentation have been described elsewhere.[16,17] A Braun linear position-sensitive detector was used along with a modified Kratky[18] collimation system and a high-temperature jumper. A wavelength of 0.154 nm was used. The beam size at the sample position was $\sim 0.2 \times 2$ mm^2. The sample-to-detector distance was 1320 mm. The detector had a receiving window width of ~ 2 mm. A special tantalum beam stop was used to stop the main beam. More details about the double-cell high-temperature jumper have been described in ref 3. The high-temperature jumper in ref 3 was modified such that some temperature precision was sacrificed in order to increase the cooling rate. Thus, the modified temperature jumper could control the temperature to ±1.5 °C, but only about 30 s was needed to cool the sample from the melt temperature to the annealing temperature. Therefore, only the first two SAXS patterns contained higher uncertainties in temperature during the temperature-transition period. The samples were melted at 220 °C for 2 min in order to avoid noticeable decomposition and changes of molecular weights. SAXS patterns were checked to make sure that the samples were indeed reduced to a state of complete segmental mixing.

Except for the absolute scattered intensity calibration, routine corrections, including attenuation, sample thickness, intensity and spatial linearity of the detector, incident intensity fluctuations, and background were performed to obtain the excess scattered intensity.

Results and Discussion

The as-reacted segmented polyurethane samples were characterized by synchrotron SAXS performed at 23 °C. Figure 1 shows the scattering patterns of PTMO-2000-PU-39 and PPO-PEO-2000-PU-39. Both curves show a scattering peak, implying the presence of a two-phase structure. The scattered intensity from PTMO-2000-PU-39 is higher than that from PPO-PEO-2000-PU-39. The integrated scattered intensity, Q, called the invariant, can be expressed by[18]

$$Q = \int_0^\infty I(q) q^2 \, dq \tag{1}$$

where I is the scattered intensity and $q = (4\pi/\lambda) \sin(\theta/2)$, with λ and θ being the X-ray wavelength and the scattering angle, respectively.

In an ideal two-phase system with sharp boundary

$$Q_i \propto \phi_1 \phi_2 (\rho_1 - \rho_2)^2 \tag{2}$$

where ϕ_i and ρ_i are the volume fraction and the electron density of the ith phase, respectively. Therefore the experimentally determined Q value divided by Q_i gives an estimate of the degree of phase separation.[19] An increased Q/Q_i value means an increased degree of phase separation. The Q/Q_i values are expressed in relative units because the instrument constant is unknown. However the values for the two polymer samples can be compared with each other since they have the same constant. An accurate evaluation of Q requires the scattering information over the entire q spacing (0 to infinity). In reality, we could only cover a finite q region. Therefore, proper extrapolations[18] have been used to correct this finite q limitation. The higher Q/Q_i value of 8.7×10^3 for PTMO-2000-PU-39 when compared with the Q/Q_i value of 4.3×10^3 for PPO-PEO-2000-PU-39 means that the degree of phase separation in PTMO-2000-PU-39 is more complete. The thermodynamic incompatibility of the hard and soft segments could be estimated by comparing the difference in the solubility parameters (δ). The calculation of Ryan et al.[20] showed δ values for PTMO, PPO, PEO, and MDI/BD to be 8.7, 8.7, 9.0, and 11.3 cal$^{1/2}$ cm$^{-3/2}$, respectively. A δ value of 8.8 cal$^{1/2}$ cm$^{-2/3}$ was estimated for the PPO–PEO used in this study. Therefore the difference in the degree of phase separation could not be explained thermodynamically based on δ values because such values for PTMO and PPO–PEO are very close to each other. In our earlier investigations[2-6] we noted that a kinetic factor was important and had to be considered. PTMO soft segment chains have no side groups and are more flexible than PPO. The kinetic barrier for PTMO is smaller than that for PPO. PTMO also has a lower glass transition temperature which implies lower intramolecular forces. Then, MDI/BD hard segments could be more readily excluded from the PTMO soft segment matrix. Although both PTMO and PPO–PEO have very similar solubility parameters, the phase separation process in PPO-2000-PU-39 could be further away from the equilibrium phase-separated state, as can be predicted by thermodynamics. This conclusion was further confirmed by our kinetics study presented next.

The hard segment interdomain spacing (d) could be estimated from the position of the scattering maximum on the basis of the equation

$$d = 2\pi/q_{max} \tag{3}$$

where q_{max} is the q value at the scattering peak. The d values without the Lorentz correction showed 17.3 nm for PTMO-2000-PU-39 and 15.0 nm for PPO-PEO-2000-PU-39. After the Lorentz correction, i.e., by multiplying I with q^2, the d values were found to be 12.6 nm for PTMO-2000-PU-39 and 12.2 nm for PPO-PEO-2000-PU-39.

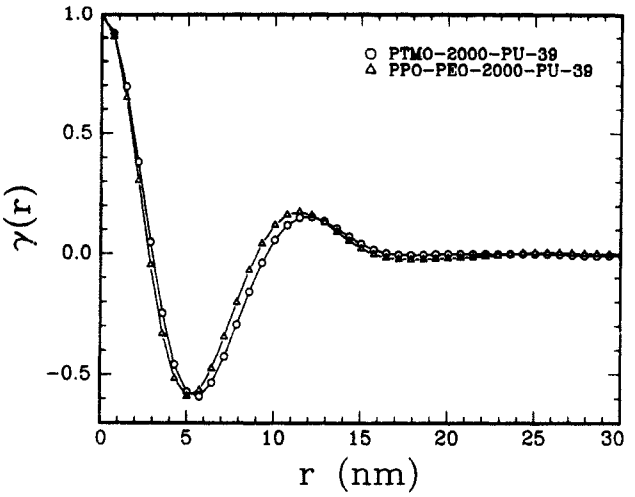

Figure 2. One-dimensional correlation functions of as-reacted PTMO-2000-PU-39 and PPO-PEO-2000-PU-39 samples.

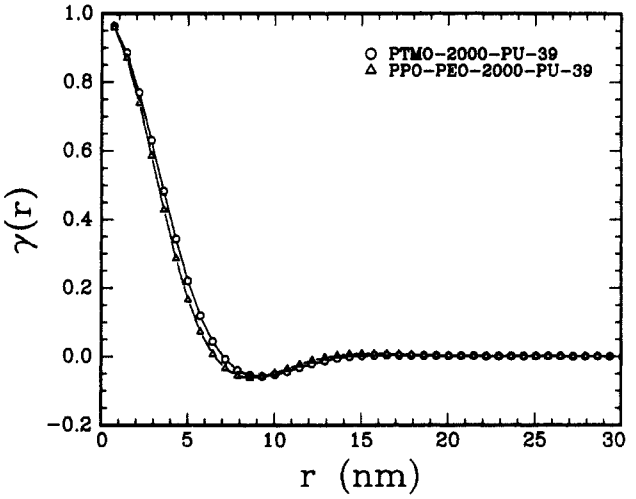

Figure 3. Three-dimensional correlation functions of as-reacted PTMO-2000-PU-39 and PPO-PEO-2000-PU-39 samples.

A more direct way is to use the correlation function analysis.[18] The one-dimensional correlation function $\gamma_1(r)$ is defined by[18]

$$\gamma_1(r) = (1/Q)\int_0^\infty q^2 I(q) \cos(qr)\, dq \qquad (4)$$

The results, as shown in Figure 2, revealed a periodic structure in both samples. The quick disappearance of the oscillation in $\gamma_1(r)$ is caused by the broad distribution in the interdomain spacing. Although there was a substantial difference in the degree of phase separation, the one-dimensional correlation functions showed little difference, indicating a similarity in the geometric structure of the two samples. The interdomain spacing from the position of the first non-zero maximum was 12.2 nm for PTMO-2000-PU-39 and 11.5 nm for PPO-PEO-2000-PU-39, in fairly good agreement with those data (12.6 and 12.2 nm) based on the Lorentz correction.

The three-dimensional correlation function $\gamma_3(r)$ is defined by[18]

$$\gamma_3(r) = (1/Q)\int_0^\infty q^2 I(q)[\sin(qr)/(qr)]\, dq \qquad (5)$$

Figure 3 shows a more diffuse maximum for both samples. The interdomain spacing (d) values for PTMO-2000-PU-39 and PPO-PEO-2000-PU-39 are in qualitative agreement with the d values without the Lorentz correction. However, the three-dimensional correlation functions did not show an exponential decay; i.e., the systems were not random.

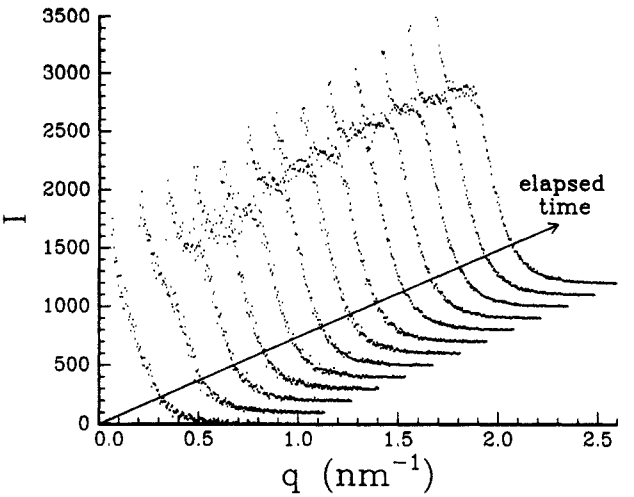

Figure 4. Time dependence of SAXS profiles by quenching the homogeneous melt of PTMO-2000-PU-39 from 220 to 131 °C. The scattered intensity showed a monotonic increase with increasing elapsed time. The elapsed time was counted immediately after the sample was jumped from the melting cell (220 °C) to the measuring cell (131 °C). From left, the curves represent, respectively, the SAXS profiles at the elapsed time of 10, 35, 56, 79, 103, 145, 209, 370, 516, 816, 1151, 2310, and 3522 s. After several preliminary tests, we found that phase separation did not proceed at the same rate during the whole process. Therefore, we chose to use varying exposure times in order to get the best signal-to-noise ratio. At the initial stage of the phase separation, the exposure time was 20 s to accommodate the rapid phase separation process. The exposure time was increased (up to 300 s) as the phase separation slowed down considerably at later stages. The elapsed time indicated above represents the time period between jumping the sample to the lower annealing temperature and the midpoint time of the data collection period in the SAXS profile. This method was also used for the results presented in Figure 5. The sample thickness was not normalized. However since it remained unchanged throughout the whole process, it did not affect our conclusions.

For segmented polyurethanes with the hard segment content used in this study, it is generally believed that the phase structure has a lamellar (or layered) structure, at least on a localized scale.[1] Together with the results from our previous investigations,[2-6] we believe that the one-dimensional correlation function and the Lorentz correction are more appropriate approaches for analyzing the data of the present two systems.

Figure 4 shows the time-dependent SAXS patterns of the PTMO-2000-PU-39 melt obtained by quenching it from 220 to 131 °C. The phase separation was very fast so that the first pattern we observed already showed some scattering. The application of a photodiode array detector[21] (which could be faster in the scanning measurement) did not help because the sample melt took about 30 s to reach 131 °C. Therefore the first two scattering patterns contained higher uncertainty. This problem was not as serious for PPO-PEO-2000-PU-39. Figure 5 shows the time-dependent SAXS patterns after the PPO-PEO-2000-PU-39 melt was quenched from 220 to 131 °C. The phase separation kinetics was slower when compared with that of PTMO-2000-PU-39. The first pattern showed very little scattering. In our previous study,[3] we observed that the interdomain spacing did not change during the phase separation process. Figure 6 shows a similar trend for the two samples. We noted the upturn during the initial stages. However it is hard to believe that lamellar structures have already been formed at such early stages of phase separation. Therefore the determination of interdomain spacing during the initial stages by using such methods might introduce unexpected uncertainty.

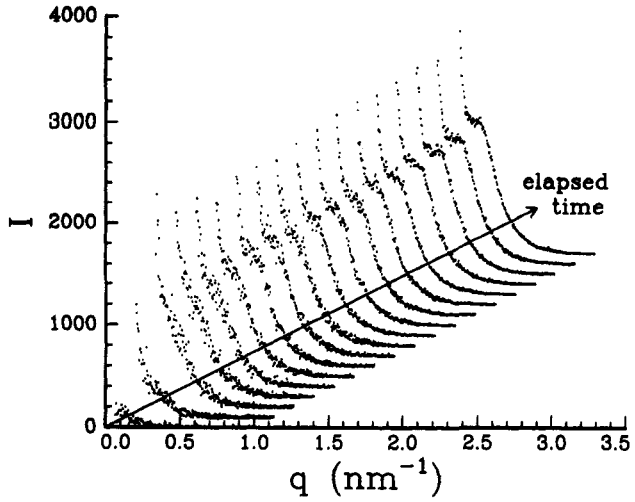

Figure 5. Time dependence of SAXS profiles after the homogeneous melt (220 °C) of PPO-PEO-2000-PU-39 was quenched to 131 °C. The scattered intensity showed a monotonic increase with increasing elapsed time. The elapsed time was counted immediately after the sample was jumped from the melting cell (220 °C) to the measuring cell (131 °C). From left, the curves represent, respectively, the SAXS profiles at the elapsed time of 10, 30, 51, 74, 97, 131, 163, 195, 228, 286, 398, 571, 750, 984, 1443, 2117, 2917, and 3705 s. The sample thickness was not normalized. However since it remained unchanged throughout the whole process, it did not affect our conclusions.

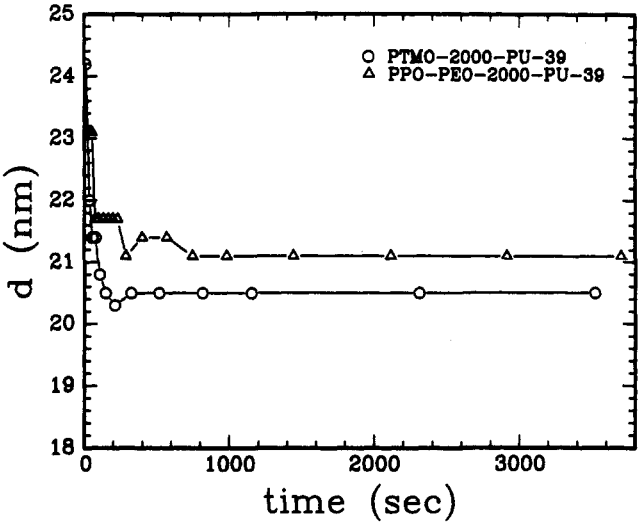

Figure 6. Time dependence of interdomain spacing (d) determined from the peak position of Iq^2 versus q.

In previous study,[3] we found that the phase separation kinetics in a segmented polyurethane could be described by an equation of relaxation with a single-relaxation time

$$X_t = (x_\infty - x_t)/(x_\infty - x_0) = \exp(-t/\tau) \quad (6)$$

where x is a physical quantity characteristic of the system. ∞, t, and 0 denote time at ∞, t and 0, respectively. τ is the relaxation time. Since Q/Q_i is an estimate of the degree of phase separation, it can be used to represent x. Thus we have

$$[(Q/Q_i)_\infty - (Q/Q_i)_t]/[(Q/Q_i)_\infty - (Q/Q_i)_0] = (Q_\infty - Q_t)/(Q_\infty - Q_0) = \exp(-t/\tau) \quad (7)$$

The relaxation times from the fitting results are 2.57×10^3, 2.35×10^2, 4.81×10^2, 2.92×10^3, and 9.18×10^3 s for PPO-PTMO-PU-50 quenched from the melt to 31, 80, 107, 135, and 167 °C, respectively.[3]

Figure 7 shows a fitting result for PTMO-2000-PU-39 with a relaxation time of 64 s. The shorter relaxation

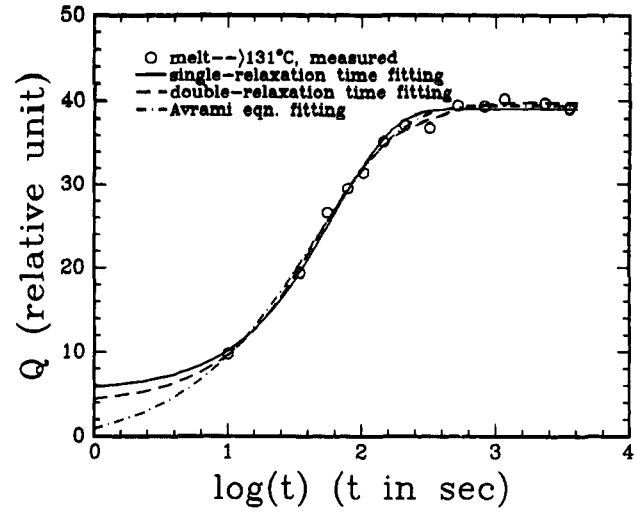

Figure 7. Fittings of different models to the experimental data (Q–t) of PTMO-2000-PU-39.

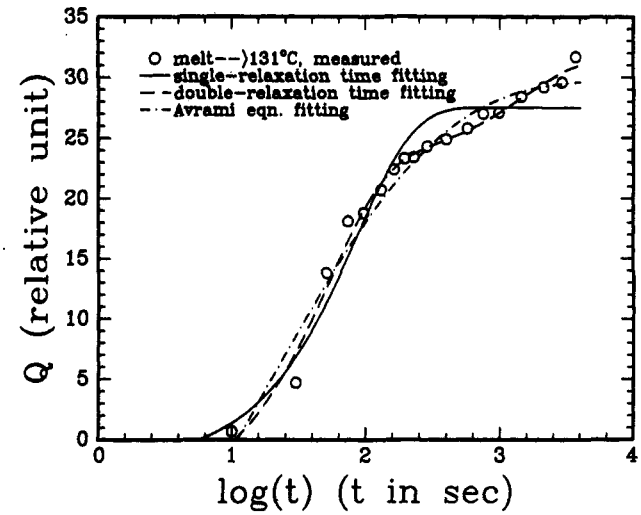

Figure 8. Fittings of different models to the experimental data (Q–t) of PPO-PEO-2000-PU-39.

time suggests that by increasing the soft segment length from 1000 to 2000, the phase separation rate is greatly increased. A longer soft segment increased the hard segment mobility due to decreased connectivity effects, whereby the hard segments became more easily excluded from the soft segment matrix. This could be the main reason for the faster phase separation kinetics for the samples with longer soft segments, strongly supporting our argument that hard segment mobility and system viscosity are the main controlling factors for the multiphase structure of segmented polyurethanes.

In order to compare different model fittings, the equation of relaxation with a double-relaxation time

$$(x_\infty - x_t)/(x_\infty - x_0) = f \exp(-t/\tau_1) + (1 - f) \exp(-t/\tau_2) \quad (8)$$

where f characterizes the fraction of τ_1, and the Avrami equation[22]

$$(x_\infty - x_t)/(x_\infty - x_0) = \exp(-kt^n) \quad (9)$$

were also used. As can be seen from Figure 7, all three models fit the experimental results fairly well. The relaxation times from the three fitting results are also in good agreement. The difference in the fittings was mainly at the very early stages, i.e., $t < 10$ s, which is, unfortunately, beyond our instrument limit. The Avrami equation is mathematically very powerful due to the presence of n. However, the power of the Avrami equation also makes

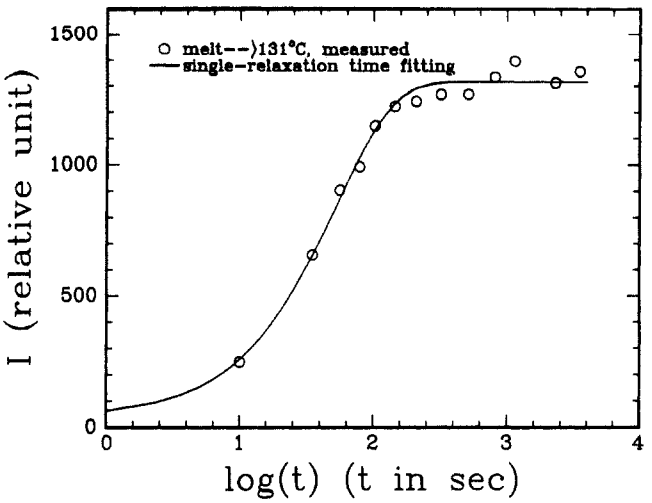

Figure 9. Time dependence of the scattered intensity at $q = 0.3$ nm^{-1} versus time for PTMO-2000-PU-39, along with model fitting.

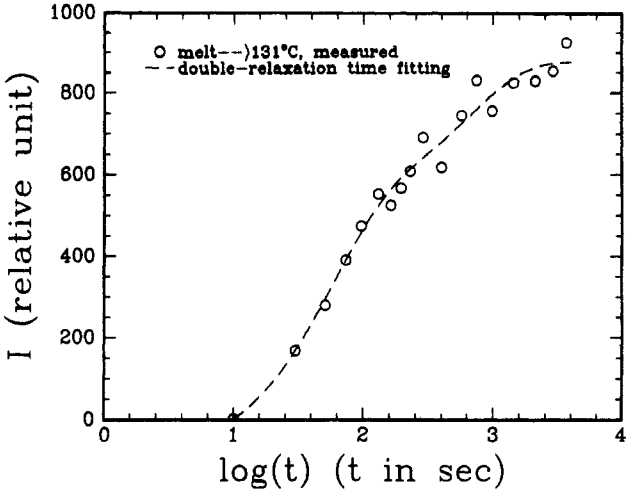

Figure 10. Time dependence of the scattered intensity at $q = 0.3$ nm^{-1} versus time for PPO-PEO-2000-PU-39, along with model fitting.

an explanation of the physical meaning of n and k more difficult and more ambiguous. The equations of relaxation with single- and double-relaxation times gave fairly good fittings. We prefer to use fittings with a single-relaxation time, because the use of double-relaxation times introduces two additional parameters which are meaningful only if the SAXS data are of extremely high quality.

Similar fittings for PPO-PEO-2000-PU-39 are shown in Figure 8. A secondary process is very obvious, while a single-relaxation time and the Avrami equation are no longer adequate. In any event, the phase separation kinetics in PTMO-2000-PU-39 and PPO-PEO-2000-PU-39 are not the same. In the study by Galambos et al.[15] where 70 wt % PPO and 30 wt % PEO were used as a soft segment, the secondary process was also obvious. In our previous study[3] where 70 wt % PTMO and 30 wt % PPO were used as a soft segment, the secondary process was not obvious at most of the annealing temperatures. Therefore, it seems that the secondary process could mainly be attributed to the characteristics of the PPO–PEO soft segment. The secondary process was also reported by Chee and Farris,[12] on the basis of the DSC results from Wilkes and co-workers[7] and from Kwei,[10] and by Lee et al.[13] using FTIR. However, we noted that the physical quantities used for the discussion of the model fitting have different meaning and might not represent the same aspect of the phase separation process. Further evidence is needed to ascertain this point. We also noted that the model fittings for PPO-PEO-2000-PU-39 suggested negative Q_0 values. A possible reason could be that we did not have high-quality data during the early stages. It could also be possible that there was an induction time on the order of ~10 s. The relaxation times from the fittings of the double-relaxation time equation are 54 s for the primary phase separation and 1.48×10^3 s for the secondary process.

The slower kinetics in the overall phase separation of PPO-PEO-2000-PU-39 when compared with that of PTMO-2000-PU-39 could again be explained by the mobility–viscosity–interaction argument. The phase structure in PPO-PEO-2000-PU-39 could be further away from the equilibrium phase-separated state due to the slow secondary process, in agreement with our results on the structure from as-reacted samples.

Our data could not be fitted well by the mechanisms of either spinodal decomposition[23-25] or nucleation and growth[26,27] due to the nonlinearity of either ln Q–t for the former or Q–t^2 for the latter.

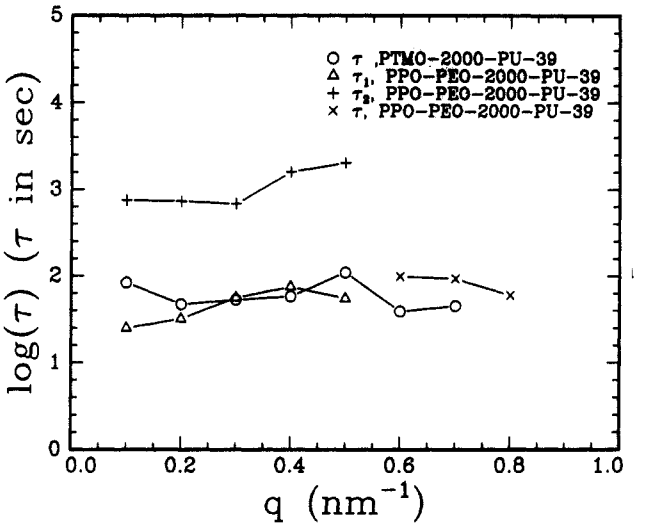

Figure 11. Values of τ as a function of scattering vector q for PTMO-2000-PU-39 (single τ) and PPO-PEO-2000-PU-39 (double τ for $q = 0.1$–0.5 nm^{-1}). The data at $q > 0.5$ nm^{-1} from PPO-PEO-2000-PU-39 could not be well fitted by the equation of relaxation with double-relaxation times. Instead, it could be fitted better by the equation of relaxation with a single-relaxation time.

The use of Q/Q_i for the quantity x could only give us the information as to how the overall system is changing with elapsed time. In order to study the phase separation kinetics using different structural scales, it is necessary to study the time dependence of scattered intensity at different q values. Figure 9 shows one such plot for PTMO-2000-PU-39 at $q = 0.3$ nm^{-1} along with the fitting of eq 4. The τ value obtained was 53 s, close to that from Q/Q_i–t. For PPO-PEO-2000-PU-39, as shown in Figure 10, the fitting shows $\tau_1 = 56$ s and $\tau_2 = 6.8 \times 10^2$ s. We want to mention that the τ values from the fitting of the I–t curves have higher uncertainty than those from the fitting of Q–t curves because the I–t curves show more high-frequency noise.

Figure 11 shows the q dependence of relaxation times. With the uncertainty of the experimental results, the τ values show little q dependence. In other words, the phase separation kinetics undergoes different structural scales with little "aggregation" effect. This is probably due to the strong effects of connectivity between the hard and the soft segments. It is noted that the relaxation with double-relaxation times could not fit the experimental

results well at $q > 0.5$ nm^{-1} for PPO-PEO-2000-PU-39. Instead, a single-relaxation time expression shows better fitting results, implying that the secondary process is significant only for large structures.

Concluding Remarks

Our mobility–viscosity–interaction argument has been tested further by using two segmented polyurethanes with a soft segment length of ~2000. As expected, the phase separation kinetics was much faster when compared with the segmented polyurethanes with a soft segment length of 1000. An equation of relaxation could still be used to describe the kinetics. However for PPO-PEO-2000-PU-39, a secondary process is obvious so that a second relaxation time has to be introduced. The effects of a kinetic factor are more significant for PPO-PEO-2000-PU-39 than for PTMO-2000-PU-39 in agreement with our previous study.[6] The interdomain spacing remained basically unchanged throughout the process. The relaxation times showed little q dependence, due to the effects of connectivity.

Acknowledgment. B.C. gratefully acknowledges the financial support of this project by the U.S. Department of Energy (Grant DEFG0286ER45237A005), the U.S. Army Research Office (Grant No. DAAL 0391G0040), and the Polymers Program of the National Science Foundation (Grant DMR8921968). The SUNY beamline at NSLS, BNL is supported by the U.S. Department of Energy (Grant DEFG0286ER45231A005). T.G. and Y.L. thank Drs. A. Darovsky, Y. Gao, and Mr. W. Lehnert for technical assistance in using the SUNY X3A2 beamline and J. Rousseau and K. Linliu for help with the SAXS data transfer.

References and Notes

(1) Gibson, P. E.; Vallence, M. A.; Cooper, S. L. In *Development in Block Copolymers-1*; Goodman, I., Ed.; Applied Science Series; Elsevier: London, 1982; p 217.
(2) Li, Y.; Liu, J.; Yang, H.; Ma, D.; Chu, B. *Polym. Mater. Sci. Eng.* **1991**, *65*, 297.
(3) Li, Y.; Gao, T.; Chu, B. *Macromolecules* **1992**, *25*, 1737.
(4) Chu, B.; Li, Y. *Colloid Polym. Sci.*, in press.
(5) Li, Y.; Gao, T.; Liu, J.; Linliu, K.; Desper, C. R.; Chu, B. *Macromolecules*, submitted for publication.
(6) Li, Y.; Ren, Z.; Zhao, M.; Yang, H.; Chu, B. *Macromolecules*, submitted for publication.
(7) Wilkes, G. L.; Wildnauer, R. *J. Appl. Phys.* **1975**, *46*, 4148.
(8) Wilkes, G. L.; Emerson, J. A. *J. Appl. Phys.* **1976**, *47*, 4261.
(9) Ophir, Z. H.; Wilkes, G. L. *Adv. Ser. Chem.* **1979**, *176*, 53.
(10) Kwei, T. K. *J. Appl. Polym. Sci.* **1982**, *27*, 2891.
(11) Camberlin, Y.; Pascault, J. P. *J. Polym. Sci., Polym. Phys. Ed.* **1984**, *22*, 1835.
(12) Chee, K. K.; Farris, R. J. *J. Appl. Polym. Sci.* **1984**, *29*, 2529.
(13) Lee, H. S.; Wang, Y. K.; MacKnight, W. J.; Hsu, S. L. *Macromolecules* **1988**, *21*, 270.
(14) Lee, H. S.; Hsu, S. L. *Macromolecules* **1989**, *22*, 1100.
(15) Galambos, A. F.; Russell, T. P.; Koberstein, J. T. *Polym. Mater. Sci. Eng.* **1989**, *61*, 359, Galambos, A. F. Ph.D. Thesis, Princeton University, 1989.
(16) Chu, B.; Wu, D.; Wu, C. *Rev. Sci. Instrum.* **1987**, *58*, 1158.
(17) Wu, D. Ph.D. Thesis, SUNY at Stony Brook, 1990.
(18) *Small Angle X-ray Scattering*; Glatter, O., Kratky, O., Eds.; Academic Press: London, 1983.
(19) Bonart, R.; Muller, E. M. *J. Macromol. Sci.—Phys.* **1974**, *B10* (1), 117.
(20) Ryan, A. J.; Stanford, J. L.; Still, R. H. *Polym. Commun.* **1988**, *29*, 196.
(21) Chu, B.; Wu, D. Q.; Howard, R. L. *Rev. Sci. Instrum.* **1989**, *60*, 3224.
(22) Avrami, M. *J. Chem. Phys.* **1939**, *7*, 1103; **1940**, *8*, 212.
(23) Nose, T. *Phase Transition* **1987**, *8*, 245.
(24) Hashimoto, T. In *Current Topics in Polymer Sciene*; Ottenbrite, R. M., Utracki, L. A., Inoue, S., Eds., Hanser: New York, 1987; Vol. II.
(25) Hashimoto, T. *Phase Transition* **1988**, *12*, 47.
(26) Lipatov, Y. S.; Grigor'yeva, O. P.; Kovernik, G. P.; Shilov, V. V.; Sergeyeva, L. M. *Makromol. Chem.* **1985**, *186*, 1401.
(27) Ryan, A. J.; Willkomm, W. R.; Bergstrom, T. B.; Macosko, C. W.; Koberstein, J. T.; Yu, C. C.; Russell, T. P. *Macromolecules* **1991**, *24*, 2883.

Registry No. MDI/BD/PTMO (block copolymer), 107678-92-2; MDI/BD/PPO/PEO (block copolymer), 111938-02-4.